Assessing the effect of alkanolamine grinding aids in limestone calcined clay cements hydration

Franco Zunino *, Karen Scrivener

Laboratory of Construction Materials, EPFL STI IMX LMC, École Polytechnique Fédérale de Lausanne, 1015 Lausanne, Switzerland

HIGHLIGHTS

- Alkanolamines enhance the aluminate reaction of LC^3 cements.
- More Hc and Mc is precipitated, increasing compressive strength.
- The addition of alkanolamines promote the hydration of ferrite and C_3A.
- The amount of aluminum and iron in the pore solution increases.
- No significant effect of TEA on calcined clay reactivity was observed.

ARTICLE INFO

ABSTRACT

Grinding aids are commonly used in cement manufacture to reduce electrostatic forces between powder particles and reduce agglomeration. Alkanolamines are known to also influence the hydration of the aluminate phases in cement. This study assessed the effect of TEA, TIPA and DEIPA addition on the hydration of LC^3 systems. It was observed that these molecules have an enhancing effect on the aluminate reaction in LC^3. They promote the hydration of ferrite and C_3A, and lead to higher amounts of hemicarboaluminate and monocarboaluminate precipitated, which contributes to porosity refinement and mechanical properties. The rate of reaction of metakaolin is not affected by the addition of TEA, independent of the iron content of the clay.

1. Introduction

The push to lower the carbon emissions associated with cement production is driving the industry to find solutions that are also technically and economically feasible. The only effective strategy to tackle this challenge is to reduce the clinker factor [1]. This has promoted the adoption of blended cements, which incorporate supplementary cementitious materials (SCMs) in addition to clinker and gypsum [2,3]. Today, blended cements are more common than traditional Portland cements.

Limestone calcined clay cements (LC^3) are a family of blended cements that incorporate limestone and calcined clays replacing part of the clinker [4,5]. Among all the materials that are commonly used as SCM, limestone and calcined clay are the only available in the quantities required for a reduction of the clinker factor on a global-scale [1]. Natural clays containing kaolinite are the

most suitable material to make LC^3 [6]. After calcination, kaolinite transforms into metakaolin, an aluminosilicate phase that can react with portlandite to form C-A-S-H and AFm [7]. Natural clays normally contain other minerals in addition to kaolinite. These associated minerals are commonly quartz, iron oxides, feldspars and other rock forming minerals [8,9].

The reactivity of blended cements depends on their mineralogical composition (clinker composition, type of SCM), but also on physical characteristics of the material, especially specific surface area [10–12]. Proper grinding is crucial to ensure a good behavior of blended cements. The different grindability of the SCMs and the clinker grains makes intergrinding challenging [13]. In general, SCMs are softer than clinker and thus will tend to overgrind while the clinker grains remain coarse [14].

Grinding aids (GAs) are incorporated during comminution of clinker to reduce electrostatic forces and minimize agglomeration of clinker and SCM grains [15]. Their chemical compositions include alkanolamines such as triethanolamine (TEA), triisopropanolamine (TIPA) and diethylisopropanolamine (DEIPA), as

---

well as glycols such as propylene glycol (PG), monoethylene glycol (MEG), and diethylene glycol (DEG). Polycarboxylate ethers (PCEs) are also commonly used as GAs. Because of their organic polar nature, GAs are preferentially adsorbed on surfaces formed by the fracture of electrovalent bonds such as Ca–O and Si–O, reducing surface energy forces [15]. This reduction leads to an increase in the fineness of the cement for a given energy consumption [15–17]. Mishra et al. showed quantitatively that the main effect of GA is the reduction of agglomeration energy [18]. Recently, it was shown that they can also improve the particle separation process of ground clays [9].

Alkanolamines are known to influence the hydration of cement in addition to improving the grinding process [19]. TEA and TIPA have been used as setting accelerators and strength enhancers [20]. Ramachadran observed that TEA could retard the hydration of the alite, but significantly accelerate the reaction of C_3A and the formation of ettringite [20,21]. In addition it has been observed that TEA can influence the solubility of fly ash [22]. TIPA has been observed to produce an increase in strength at later ages [23,24]. DEIPA can promote the formation of ettringite and the hydration of aluminate clinker phases [25].

The interaction of TEA and TIPA has been associated with the formation of amine-iron complexes. Gartner and Myers proposed that the iron complex increased the solubility of iron enough to be able to coprecipitate with aluminum to form ettringite and AFm [24]. In this study, Gartner and Myers also suggest that an amine-Al complex might be formed. Recently, an atomistic model for the TEA-Al complex has been proposed by DFT calculations [26].

Despite the extensive amount of research on the effect of different alkanolamines in pure clinker phases and OPC hydration, there are no studies that address their effect in systems where additional aluminum and iron sources are introduced, such as LC^3. This paper presents a study on the effect of alkanolamine grinding aids (TEA, TIPA and DEIPA) on the hydration kinetics and phase assemblage of LC^3. The influence of GA addition in porosity refinement and compressive strength is discussed in the light of the observed interactions of alkanolamines with iron and aluminate phases in LC^3.

2. Materials and methods

2.1. Raw materials

A commercial ordinary Portland cement (OPC) conforming to EN 197-1 as CEM I 42.5R was used in this study. Two different calcined clays were used for the preparation of LC^3 blends. First, a natural clay from Chile (Cy) with 60.3% of kaolinite as measured by TGA and a high iron content (9.44% Fe_2O_3) was selected. The clay was ground and calcined in a laboratory furnace at 800 °C for 1 h. Complete dehydroxylation of kaolinite was verified by TGA. The iron mineral after calcination corresponds to hematite. The other clay corresponds to a high purity metakaolin (MK, 95% purity from Burgess). As the content of kaolinite is higher, MK was mixed with a quartz powder (Qz) to achieve the same total kaolinite content as Cy. A commercial limestone (Omya, Durcal 5) was used.

The chemical (by XRF) and phase (by XRD/Rietveld) compositions of the raw materials are shown in Table 1. The particle size distribution (PSD) of these materials, measured by laser diffraction, is shown in Fig. 1. The optical model parameters and the dispersant were selected following the recommendations given in [27].

The specific surface area (SSA) of each raw material was measured by nitrogen adsorption, using the BET model. In all cases, samples of around 1.5 g were degassed for 2 h at 200 °C under a N_2 flux before the measurement. The specific gravity was measured using a liquid pycnometer with isopropanol as solvent.

Distribution values and specific gravities are summarized in Table 2.

Pure molecules of different grinding aids were used in this study. Three different alkanolamines were studied. Triethanolamine (TEA, SigmaAldrich 90,279 99% purity), triisopropanolamine (TIPA, SigmaAldrich 254,746 95% purity) and diethylisopropanolamine (DEIPA, SigmaAldrich 233,757 93% purity) were used. In addition, the effect of alkanolamines on LC^3 hydration was compared to other families of grinding aids. Polypropylene glycol (PPG, Mn 1000, SigmaAldrich 202320), dipropylene glycol methyl ether (DPG, SigmaAldrich 484253, 99%) and polycarboxylate ether (PCE, GCP Chemicals, ADVA 955, 60% solid content) were used. In all cases, aqueous solutions at 0.5% solid content were prepared to facilitate handling, dosing and dispersion of the grinding aids.

2.2. Mixture design

An LC^3-50 system (50% clinker content) was used as a reference to study the effect of alkanolamine GAs on hydration and mechanical properties. The clay to limestone ratio was fixed at 2-to-1. To achieve adequate sulfate balance of the systems, 1% of gypsum was added in all cases. This leads to a mixture design composed of 54% OPC, 30% calcined clay (Cy or MK + Qz), 15% LS and 1% gypsum. A water to binder ratio (w/b) of 0.4 was used.

The addition of grinding aids to the LC^3 systems was conducted starting from the 0.5% solid content solutions prepared. The necessary amount of solution was incorporated to the mixing water before casting to achieve 100 or 200 parts per million (ppm), (0.01 and 0.02% respectively) referred to the mass of binder. These dosages are common concentrations for this type of molecules when used as grinding aids. In the case of TEA, some experiments were conducted at higher concentrations. The water addition due to the incorporation of the GA solutions was computed and subtracted from the mixing water. LC^3 paste samples were prepared by mixing the water plus the GA with the powders using a vertical axis high shear mixer, at 1600 rpm for 2 min.

2.3. Experimental methods

The heat evolution was measured in a TAM Air isothermal calorimeter at 20 °C for up to 7 days. From the paste samples prepared, 10 g of was placed in a glass ampoule, sealed and introduced in the calorimeter.

X-ray diffraction (XRD) measurements were carried out on freshly cut slices of hardened paste at 1, 2, 3, and 7 days of hydration to follow the hydration of the clinker phases and the formation of aluminate hydrates in the systems. Rietveld refinement was conducted using the HighScore Plus v4.8 software. The slices were analyzed in a Bragg-Brentano configuration in a PANalytical X'pert pro diffractometer working at 45 kV and 40 mA with a copper source. A 1/2° soller slit was used, and scans were acquired between 7 and 70° 2θ in 14 min, equivalent to a step size of 0.0167° 2θ. The external standard method was used to compute the K-factor of the device and account for the amorphous phases present. A scan of a rutile standard was acquired in the same conditions after the experiments for this purpose.

Porosity measurements were conducted by mercury intrusion porosimetry (MIP) in paste samples at 1 and 7 days. Slices similar to the ones prepared for XRD were immersed in isopropanol for 7 days to arrest the hydration. Afterwards, they were stored in a desiccator for at least 48 h to remove the remaining isopropanol. About 1 g of hardened paste was placed in a glass dilatometer crushed into 4 to 5 pieces. Intrusion was conducted up to a pressure of 440 MPa. A contact angle of 120° was assumed between mercury and the cement paste.

Table 1
Chemical (from XRF) and phase composition (from XRD) of OPC, MK, Cy, LS and Qz.

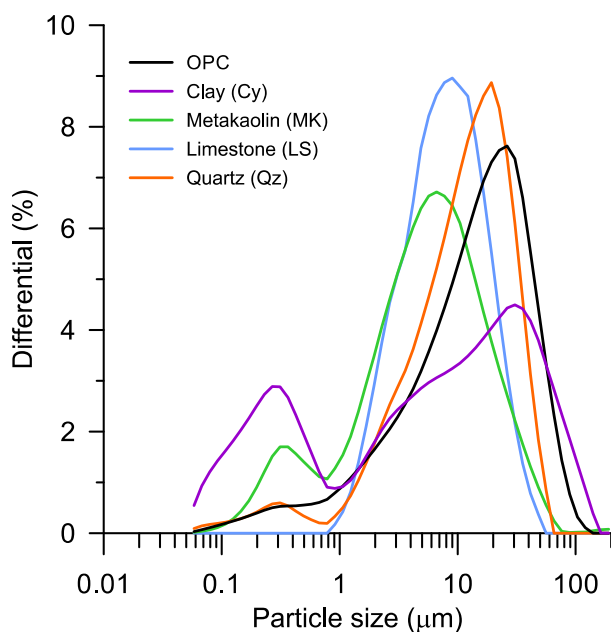|	OPC	MK	Cy	LS	Qz
SiO_2	19.51	52.00	48.13	0.11	99.83
Al_2O_3	4.42	43.80	35.08	0.00	0.00
Fe_2O_3	3.12	0.33	9.44	0.04	0.03
CaO	63.85	0.03	0.81	54.96	0.02
Na_2O	0.19	0.14	0.20	0.06	0.00
K_2O	0.83	0.29	0.08	0.00	0.05
MnO	0.05	0.01	0.01	0.00	0.00
TiO_2	0.31	1.53	2.27	0.00	0.02
MgO	2.10	0.01	0.52	0.15	0.00
P_2O_5	0.33	0.16	0.34	0.00	0.00
SO_3	3.25	0.10	0.02	0.03	0.00
LOI	1.54	1.47	2.98	42.5	0.02
C_3S	66.5	–	–	–	–
C_2S	4.0	–	–	–	–
C_3A	4.9	–	–	–	–
C_4AF	9.6	–	–	–	–

Fig. 1. Particle size distribution of the raw materials used in this study.

Paste samples were also used to assess compressive strength. Cubic samples of 2 cm were prepared and stored in sealed conditions until testing. Strength measurements were conducted at 1, 2, 3, 7, 14 and 28 days of hydration, using a 60 kN load cell with a 1 N resolution and a loading rate of 0.4 kN/s.

The aluminum and iron content were measured in pore solution samples collected at 1, 2, 3 and 7 days of hydration in LC^3 systems incorporating 200 and 500 ppm of TEA. The pore solution extraction was done in a cylindrical paste sample using a pore press device at 600 kN for 7 min. Samples were filtered using a 0.2 μm syringe filter after collection. pH was measured right after extrac-

tion. Afterwards, a 3 times dilution in 1% HNO_3 was prepared. The measurements were conducted using inductively coupled plasma optical emission spectrometry (ICP-OES).

The microstructural development was studied using scanning electron microscopy (SEM), using a FEI Quanta 200 microscope. Element distribution maps were collected from polished sections of LC^3 paste (from the same discs as for MIP measurements) embedded in resin, using an accelerating voltage of 12 kV, working distance of 12.5 mm and a spot size adjusted to obtain about 0.9nA of current over the sample. The maps were collected at 1000x magnification in 30 cycles with a dwell time of 512 μs, resulting in a total measuring time of approximately 8 h per map. The obtained data was then quantified using a calibration database acquired under the same conditions. Afterwards, the edxia image analysis framework was used to process the hyperspectral maps and obtain phase distribution masks [28].

3. Results and discussion

3.1. The effect of TIPA, TEA and DEIPA addition in LC^3 properties

Calorimetry curves obtained for LC^3 systems with Cy (iron-rich) clay incorporating 100 and 200 ppm of alkanolamines are shown in Fig. 2. A significant enhancement of the aluminate peak is observed, with higher maximums of the peaks for the higher dosages of GA. DEIPA exhibits the highest enhancement, followed by TEA and TIPA.

In the case of TEA (both addition levels) and DEIPA at 200 ppm a shortening of the time to reach the onset of the aluminate peak is observed. As it has been previously shown [29], the sulfate balance of blended cements is influenced by the rate of sulfate adsorption in C-A-S-H. In addition, the amount of ettringite precipitated during the alite peak can also modify the position of the aluminate peak [30]. In this case, the alite peaks appear similar in all cases, which suggests that the acceleration of the aluminate peak is linked to a higher amount of ettringite being precipitated before

Table 2
Distribution values, span (width), specific surface area and specific gravity of raw materials.

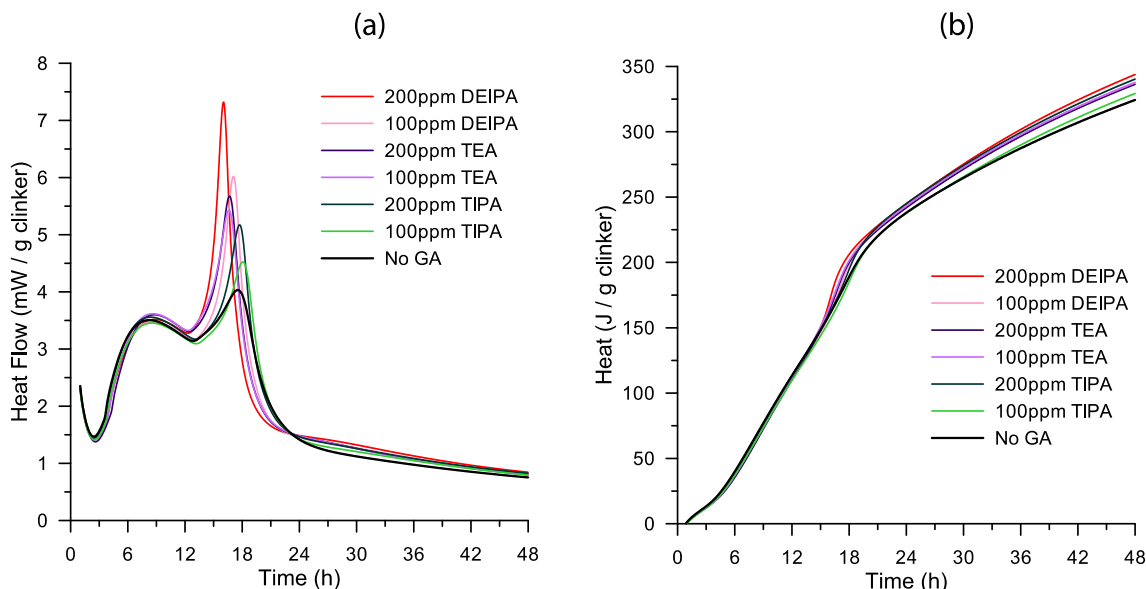|	OPC	MK	Cy	LS	Qz
D_V90 (μm)	41.42	20.17	56.22	19.3	11.96
D_V50 (μm)	14.22	5.13	7.72	7.71	4.56
D_V10 (μm)	1.67	0.54	0.17	2.27	0.36
Span (−)	2.80	3.83	7.26	2.21	2.54
SSA (m²/g)	1.41	13.56	47.16	2.39	3.45
Sp. Gravity (g/cm³)	3.09	2.20	2.61	2.71	2.65

Fig. 2. Heat flow (a) and total heat (b) curves of LC^3-50 systems with Cy clay and alkanolamine GA additions.

the onset. Ramachandran previously showed that TEA accelerates the reaction rate of C$_3$A [20,21] with a consequent increase in the precipitated ettringite.

Fig. 2b shows the corresponding total heat for the different LC^3 systems studied. Despite the clear differences in the aluminate peaks observed in Fig. 2a, the total heat curves appear similar for DEIPA, TEA and the system with 200 ppm TIPA at 48 h. Thus, despite the clear peak shape difference, the amounts of ettringite precipitated in these systems is expected to be similar.

Calorimetry curves of LC^3 systems incorporating 100 and 200 ppm of glycol-based (PPG and DPG) and PCE-based GAs are shown in Fig. 3. In this case, no significant effect of the grinding aids on the hydration kinetics of LC^3 systems is observed. The total heat release is in all cases similar to the system without the addition of grinding aids. While all these molecules have proven effec-

tive in improving the grinding efficiency of calcined clays [31] and the particle classification process after grinding [9], they do not influence the hydration kinetics of LC^3-type systems at the addition levels explored.

The enhancement observed with the addition of alkanolamines in the aluminate peak of LC^3 systems show that these molecules can influence the hydration kinetics of these blended systems. To better understand the effect of alkanolamines in LC^3, experiments were conducted to assess the influence of these molecules on OPC hydration kinetics. Fig. 4 shows a heat flow curve of plain OPC, and also with 200 ppm of addition of DEIPA and TEA, molecules that exhibited the strongest enhancement effects in the aluminate reaction of LC^3 (Fig. 2).

A reduction of the slope of the acceleration stage of the alite peak is observed in both systems incorporating GAs. Furthermore,
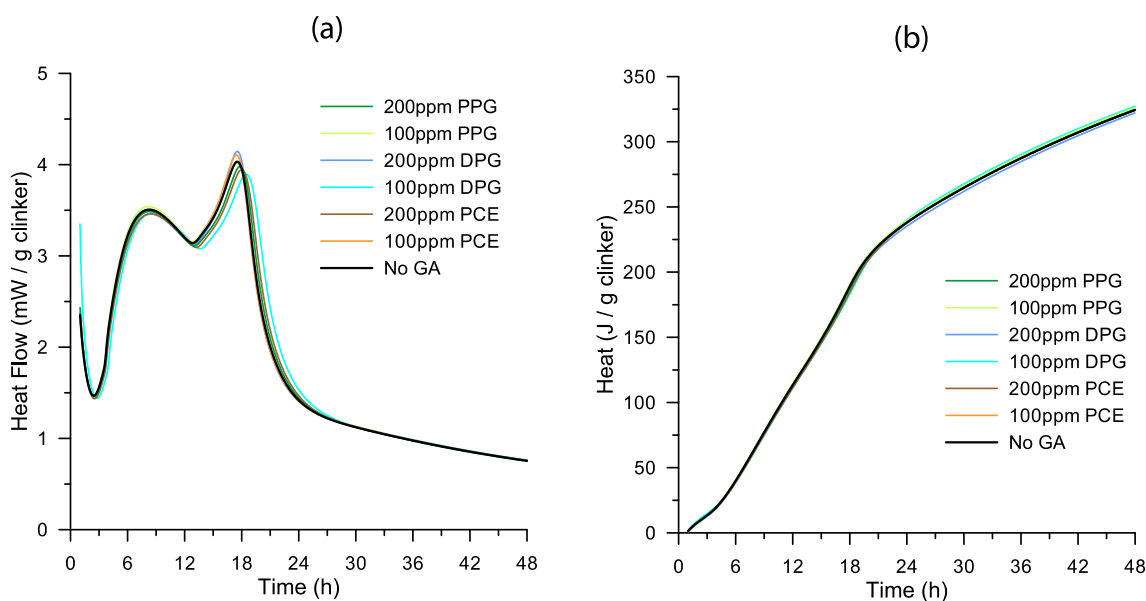

Fig. 3. Heat flow (a) and total heat (b) curves of LC^3-50 systems with Cy clay and glycol-based/PCE GA additions.
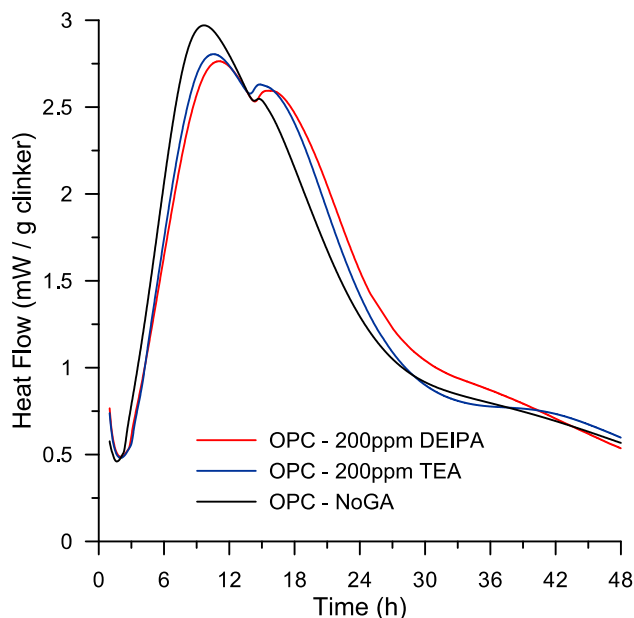
Fig. 4. Heat flow curve of OPC with addition of 200 ppm of DEIPA and TEA.

the height of the alite peak is reduced as compared to the plain OPC system. This could be related with a higher degree of reaction of C_3A/ferrite in the presence of these alkanolamines.

The reduction in slope of the acceleration period is not observed in the LC^3 systems, Fig. 2. Moreover, the height of the alite peaks is similar among all systems with GA as compared to the control LC^3 system. It can be inferred that the addition of limestone and calcined clay in LC^3 provides sufficient enhancement of the alite reaction through filler effect to offset the negative effects observed in OPC.

Considering the position of the maximum of the alite peak in each case as a reference, the onset of the aluminate peak also occurs earlier (i.e., at a lower DoH of alite) in the OPC systems with TEA and DEIPA. This further supports the observation regarding more sulfate being consumed during the acceleration period due to an increased rate of reaction of C_3A and/or ferrite. The aluminate peaks also appear enhanced compared to the control OPC system.

Fig. 5 shows the compressive strength of LC^3 systems measured in paste samples. TEA, TIPA and DEIPA have positive effects in mechanical properties but in different amounts and at different hydration times. TEA and DEIPA show increases in strength com-
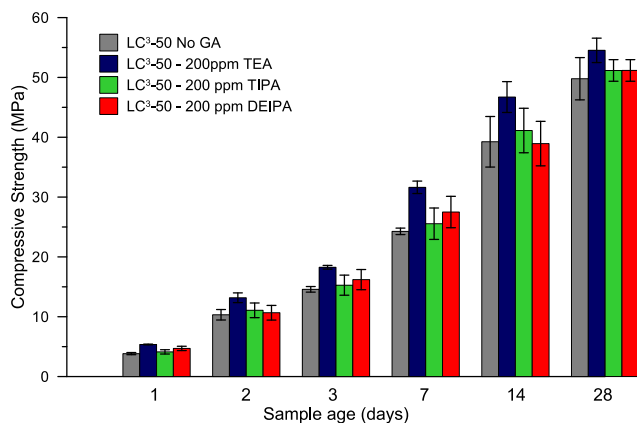
pared to the control system at early ages, TEA being significantly higher. TIPA shows similar strength at early ages, but it improves in the long term, in general agreement with previous studies [20]. Among the 3 alkanolamine molecules used, TEA appears to have the highest potential to increase the strength of LC^3-type systems.

The porosity measured by MIP of the same systems shown in Fig. 5 are presented in Fig. 6 at 1, 3 and 7 days of hydration (total porosity in Fig. 5a, 5b and 5c and size distributions in Fig. 5d, 5e and 5f). At 1 day, the system with TEA exhibits the smallest critical entry radius, while the system with DEIPA shows the lowest total porosity. DEIPA and TIPA have a similar critical entry radius to the control system. In general, all systems show similar pore size distributions. At 3 days of hydration, TEA and DEIPA systems show a more refined structure as compared to TIPA and Control, as evidenced by their smaller critical entry radius. This is consistent with the strength results observed at this age. At 7 days, all the systems incorporating grinding aids have a lower critical entry radius than the control system. The finer fraction (below 10 nm) of the pore size distributions is similar among all systems.

To understand the origin of the refined porosity and increased strength observed in the LC^3 systems with alkanolamines, the degree of hydration of the main clinker phases and the phase assemblage was characterized by XRD. Fig. 7 show the DoH of alite, C_3A and ferrite, and Fig. 8 the quantification of ettringite and hemicarboaluminate plus monocarboaluminate (Hc + Mc) for each system.

The DoH of alite is slightly lower in the systems incorporating GAs at 24 h. At later ages, the differences between systems with and without alkanolamines is negligible. The DoH of C_3A is higher at 24 h for the systems incorporating alkanolamines. Afterwards, an enhanced hydration for C_3A is observed in the systems with TEA and DEIPA. This agrees with previous observations on C_3A hydration using TEA [21]. In this study, DEIPA appears to have a similar effect, although less intense than TEA.

The DoH of ferrite (C_4AF) is significantly higher at 24 h in all systems with GA additions. At 7 days, the system incorporating 200 ppm of TIPA depletes anhydrous ferrite, while the systems with DEIPA and TEA reach DoH values around 90% for this phase. In contrast, the control system reaches 74% DoH of ferrite at the same age. The higher DoH observed in the ferrite phase when alkanolamines are incorporated could be attributed to the formation of amine-iron and amine-aluminum complexes at high pH [24]. The increased mobility of iron and aluminum in the systems with alkanolamines might explain the higher degrees of reaction observed.

The amount of ettringite is similar among all systems, as the limiting factor is the availability of sulfate. However, the amounts of Hc and Mc precipitated are significantly higher in the systems with alkanolamines. The highest amounts are observed in the system with TEA, followed by DEIPA and TIPA. This corresponds with the trend observed in compressive strength, Fig. 5. Recently, it has been shown that the contribution of Hc and Mc in LC^3 strength and porosity refinement is significant [32,33]. Thus, the enhanced precipitation of these phases could explain the increased strength observed in LC^3 systems incorporating these molecules.

3.2. Further insights on the influence of TEA in LC^3 hydration

Since TEA was the molecule that exhibited the highest enhancement of strength in LC^3 system, the interactions of this molecule with LC^3 were studied in more detail. Fig. 9 shows the concentration of iron and aluminum in the pore solution of an LC^3 system with 0, 200 and 500 ppm of added TEA. In this case, the MK + Qz clay (no iron) was used to study the effect of TEA addition on mobilization of iron from ferrite alone.
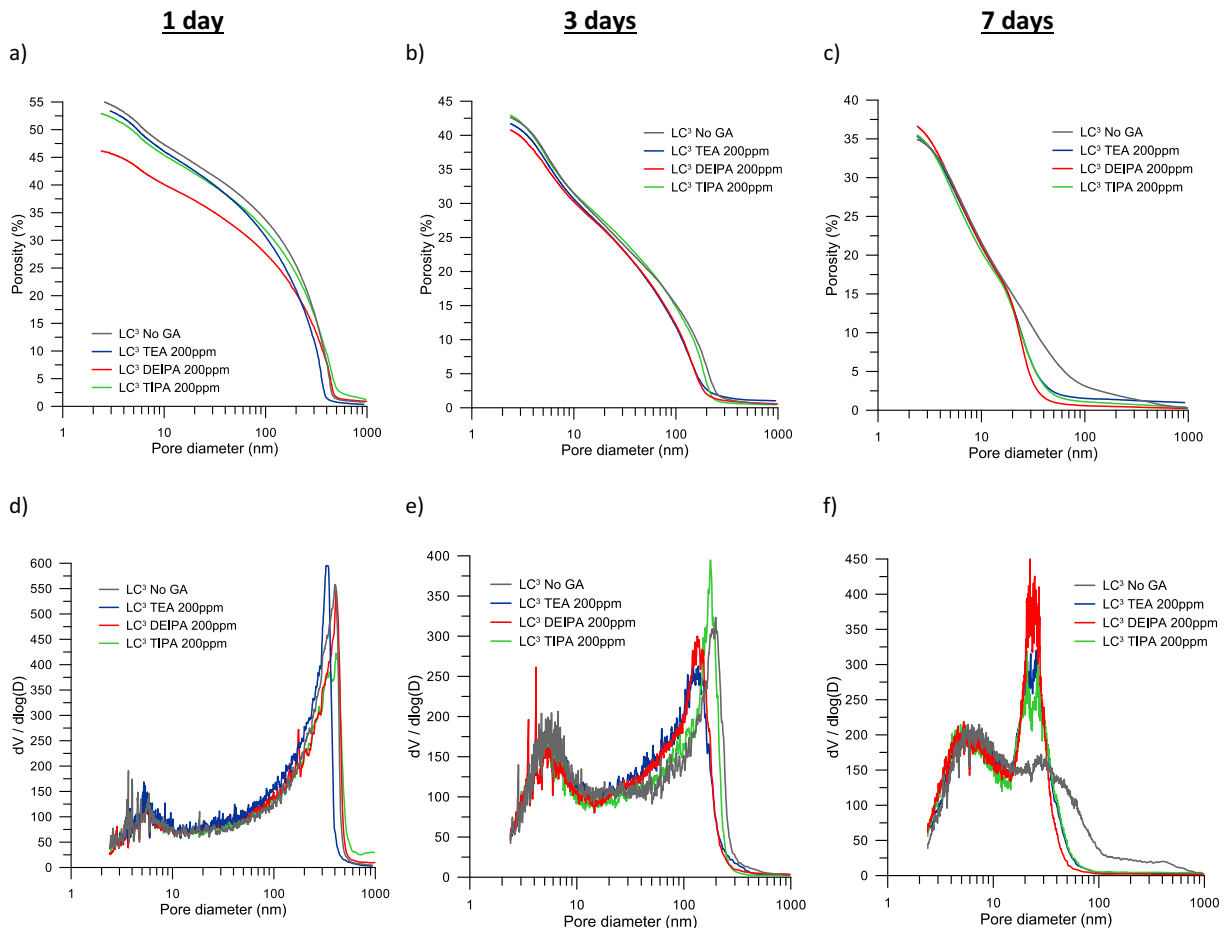

Fig. 5. Compressive strength of LC^3-50 paste samples incorporating 200 ppm of TEA and DEIPA.

Fig. 6. Total porosity (a, b, and c) and pore size distribution (d, e and f) of LC^3-50 paste samples incorporating 200 ppm of TEA, TIPA or DEIPA at 1, 3 and 7 days of hydration. Contact angle assumed 120°.
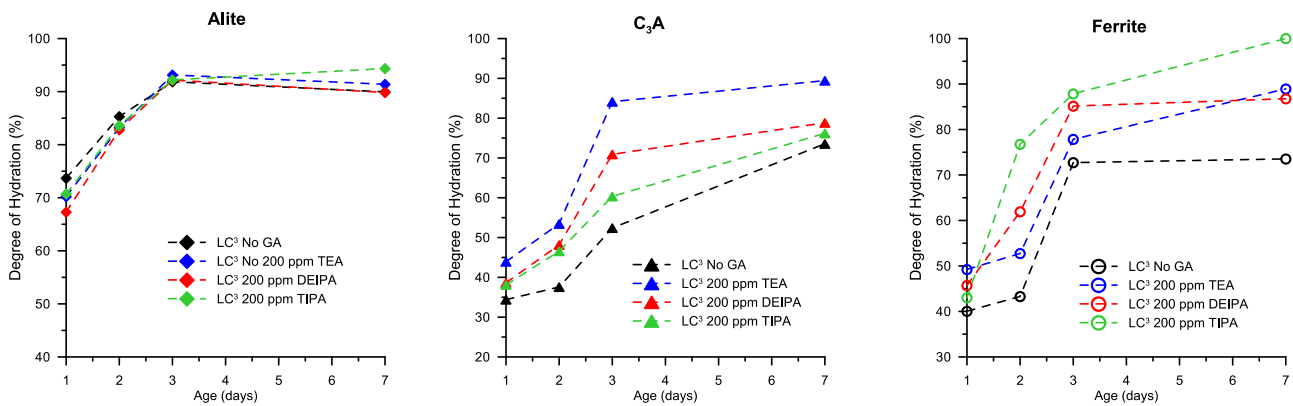

Fig. 7. DoH of alite, C$_3$A and ferrite in LC^3-50 systems incorporating alkanolamine GAs.

At 24 h of hydration, the concentration of aluminum increase with increasing amounts of TEA. Afterwards, the difference between the systems with TEA and the control system is minor. In the case of iron, it was only detected after 2 days of hydration in the system with TEA. In the control system, the measured values were always below the detection limit of 0.055 mmol/L. The content of iron in solution increases with an increase in the amount of TEA added. These observations are in good agreement with the higher degrees of reaction of ferrite measured by XRD, Fig. 7.

The pH of the system with 500 ppm was slightly higher at 24 h. Overall, it can be stated that TEA does not seem to accelerate the reaction of metakaolin in the same way as ferrite and possibly C$_3$A during the first 24 h. In addition, as the degree of reaction of alite in the systems with TEA is expected to be slightly lower than the control (Fig. 7), the measured pH values further confirm that metakaolin is indeed reacting at the same rate or slightly slower in the systems with TEA.

Based on the previous results, there is a clear interaction between TEA and iron in LC^3 systems. However, there is still an
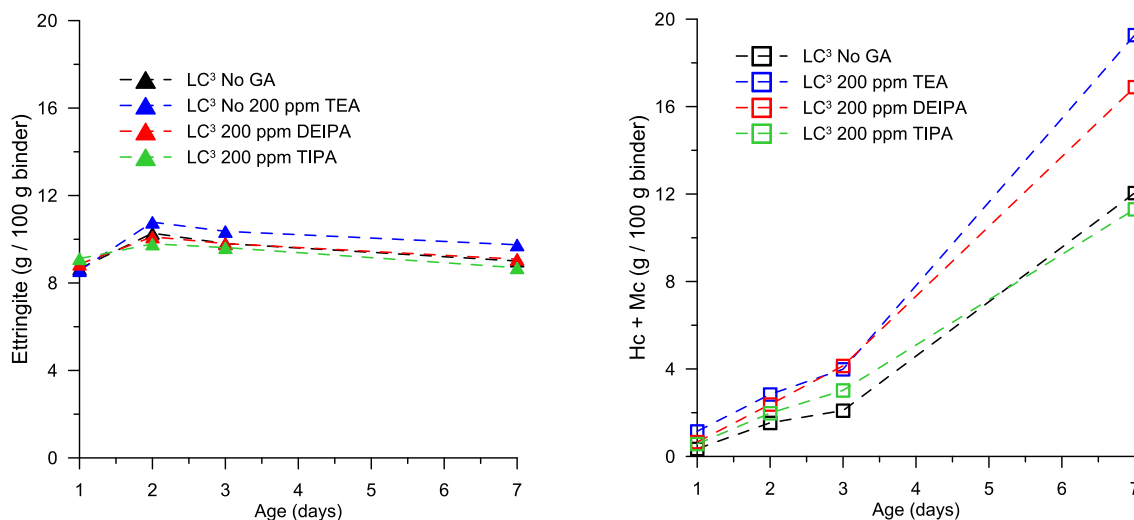
Fig. 8. Ettringite and Hc + Mc content evolution in LC^3-50 systems incorporating alkanolamine GAs.
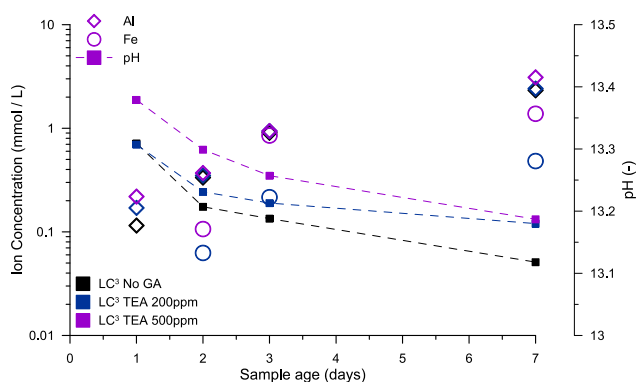

Fig. 9. pH, aluminum and iron concentration in pore solution of LC^3-50 (MK + Qz clay) paste systems incorporating TEA.

open question if this interaction is limited to ferrite or also affects the iron phases present in the calcined clay fraction as part of the impurities of natural clays.

A series of isothermal calorimetry experiments were performed with the aim to clarify this question. The sources of iron from an LC^3 system were removed one by one, and the effect of TEA and DEIPA in the observed enhancement of the aluminate peak was measured. A system with Cy clay and gray cement (iron from ferrite and calcined clay), another with gray cement and MK + Qz (iron only from ferrite) and a third one with white Portland cement and MK + Qz clay (no iron in the system) were compared. The results are shown in Fig. 10.

The enhancement of the aluminate peak observed in the systems containing gray cement and Cy clay (Fig. 10a and Fig. 2) is also observed in the systems with gray cement and MK + Qz clay (Fig. 10b). This shows that the presence of iron in the calcined clay is not necessary for the enhancement to take place. This agrees with the pore solution results, where the same synthetic clay without iron (MK + Qz) was used to prepare the samples and an increase in the iron concentration was observed.

However, when the iron phase from cement (ferrite) is also removed, the situation changes. As seen in Fig. 10c, the aluminate peaks between the control system and the ones incorporating TEA and DEIPA are similar, and no clear enhancement is observed. Thus, a major part of the observed enhancement of the aluminate peak in

LC^3 systems incorporating alkanolamines appears to be associated with an accelerated hydration of ferrite. Nevertheless, the aluminate peaks of the systems with TEA and DEIPA in Fig. 10c are still slightly higher than the control. This could be due to a promoted reaction of C$_3$A (still present in white cement) by the addition of TEA and DEIPA [21].

To further explore the influence of TEA in the rate of reaction of metakaolin, the R^3 test [34] was used, as it allows to assess the intrinsic reactivity of the clay independently of the cement used. Furthermore, high correlation of this test with compressive strength results have been observed. Both clays, MK (no iron) and Cy (high iron content) were tested, in one case with the standard R^3 solution and in other with the addition of 500 ppm (referred to the total solids) TEA. The total heat curves obtained are shown in Fig. 11.

The addition of TEA in the MK clay has no effect in the observed reaction kinetics. The difference with the control system is within the expected variability of this test. In the case of the high iron clay (Cy), a slight increase in the early reaction rate is observed between 12 and 30 h in the system with 500 ppm TEA. However, the difference is small and the system without the addition of TEA reaches an equivalent degree of reaction afterwards. Both results agree with the pH values observed in Fig. 9. Moreover, it indicates that the enhancements observed in Fig. 10 are mainly due to the enhanced reactivity of ferrite and C$_3$A rather than metakaolin.

The effect of TEA additions on the reaction of alite was further studied with higher additions of admixture. Fig. 12 shows the heat flow curves of LC^3 systems with MK + Qz clay and additions of TEA up to 2000 ppm. Higher additions of TEA lead to more enhancement of the aluminate peak. However, the slope of the acceleration period of the alite peak decreases with increasing amounts of TEA above 200 ppm. As previously discussed, this could be explained by the increased amount of aluminum in the systems with TEA during the first hours of hydration.

Among the systems with TEA, the position of the onset of the aluminate peak appears to remain constant. As more aluminum is available in the pore solution, more ettringite is formed during the acceleration period of alite and consequently, more sulfate is consumed. On the other hand, alite reacts at a slower rate as the TEA concentration increases, and therefore the amount sulfate adsorbed into C-A-S-H decrease [29]. These two simultaneous effects seem to offset each other and overall, the onset of the aluminate reaction is not affected. However, as the slope of the accel-
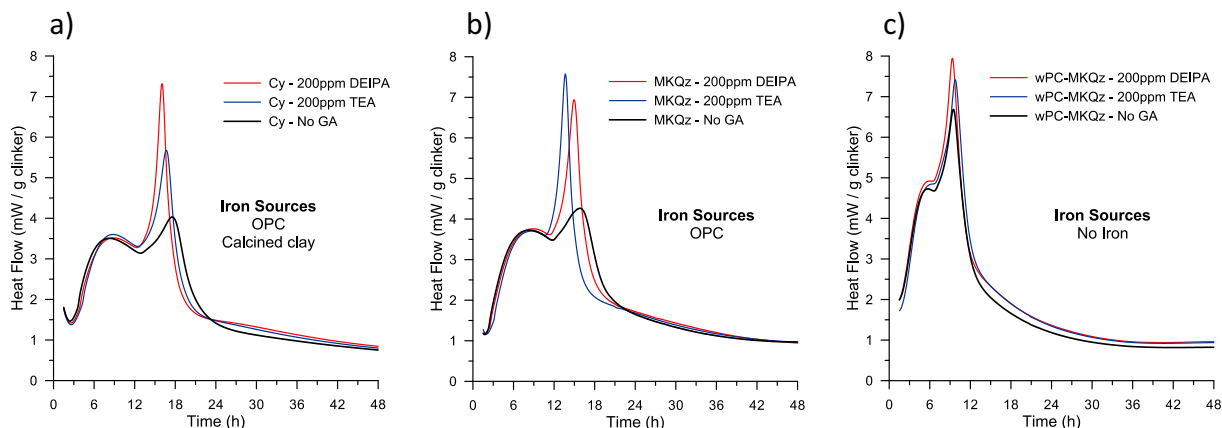
Fig. 10. Heat flow curves of different LC^3-50 systems with additions of TEA and DEIPA and iron phases in cement and calcined clay (a), only cement (b) and neither cement or calcined clay (c).
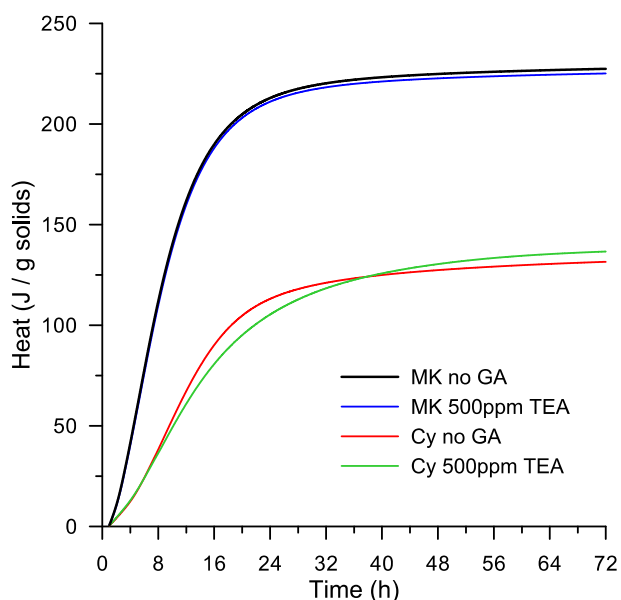

Fig. 11. R^3 test total heat curves of Cy and MK clays with and without the addition of 500 ppm TEA.

Fig. 12. Heat flow curves of LC^3-50 systems (MK clay) with higher additions of TEA.

eration period goes down the position of the alite peak also shifts right. Consequently, for the highest dosage of TEA (2000 ppm) the system appears slightly undersulfated.

TEA lead to the highest increase in strength, as seen in Fig. 5. The three alkanolamines have different effects on clinker hydration and the precipitation of hydrates, as seen in Fig. 7 and Fig. 8. Higher amounts of hydrates formed lead to a higher degree of porosity refinement. On the other hand, the molar mass of TEA (149.2 g/mol) is lower compared to TIPA (191.3 g/mol) and DEIPA (163.2 g/mol). This implies that at constant mass additions, as in this study, more molecules are added in the case of TEA. Consequently, higher surface coverages can be expected. This difference could also contribute to the observed differences in the behavior of TEA, DEIPA and TIPA.

3.3. Microstructure of LC^3 incorporating TEA

To study the effects of the addition of TEA in the microstructure of LC^3, an hyperspectral element map of an LC^3 system with MK + Qz clay was collected for a control (No GA) and 500 ppm sys-
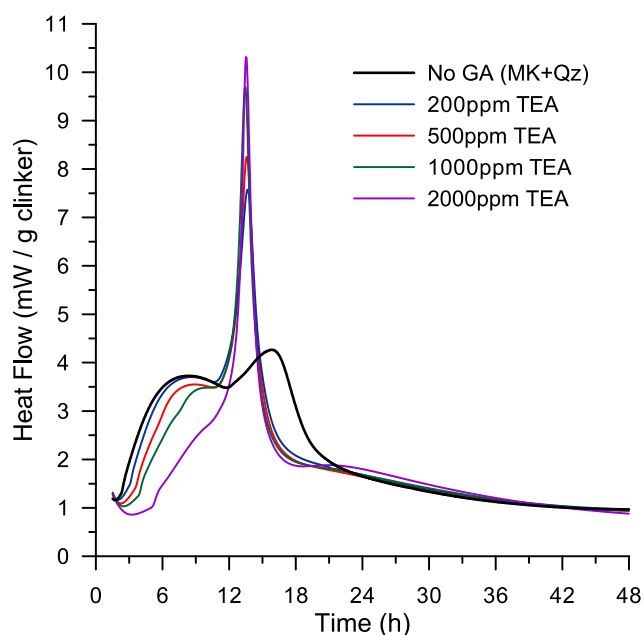
tem at 7 days of hydration. The data obtained was analyzed with *edxia* [28], and composite micrographs were produced to assess the distribution of hydrated phases, particularly Hc and Mc. The composition of each individual point of the map is presented as scatter plots of element composition expressed as Al/Ca vs Si/Ca ratio in Fig. 13a and Fig. 13b for control and TEA 500 ppm systems, respectively.

In the datasets collected for the control system, iron appears distributed in the microstructure. No other iron-bearing hydrates were observed in significant quantities. The AFm points were identified and are shown as a color mask in Fig. 14.

As observed in the XRD results (Fig. 8), more Hc and Mc was observed with the addition of TEA. This is clearly observed in the composite micrograph shown in Fig. 15 for the 500 ppm TEA system. The computed are fraction of AFm (Hc + Mc) in the No GA system was 2.3%, while in the 500 ppm one it was 6.2%. No clear iron-bearing hydrated phase is observed in this case as in the control system.

From a microstructural point of view, the main effect of TEA addition in LC^3 is associated with a higher precipitation of Hc
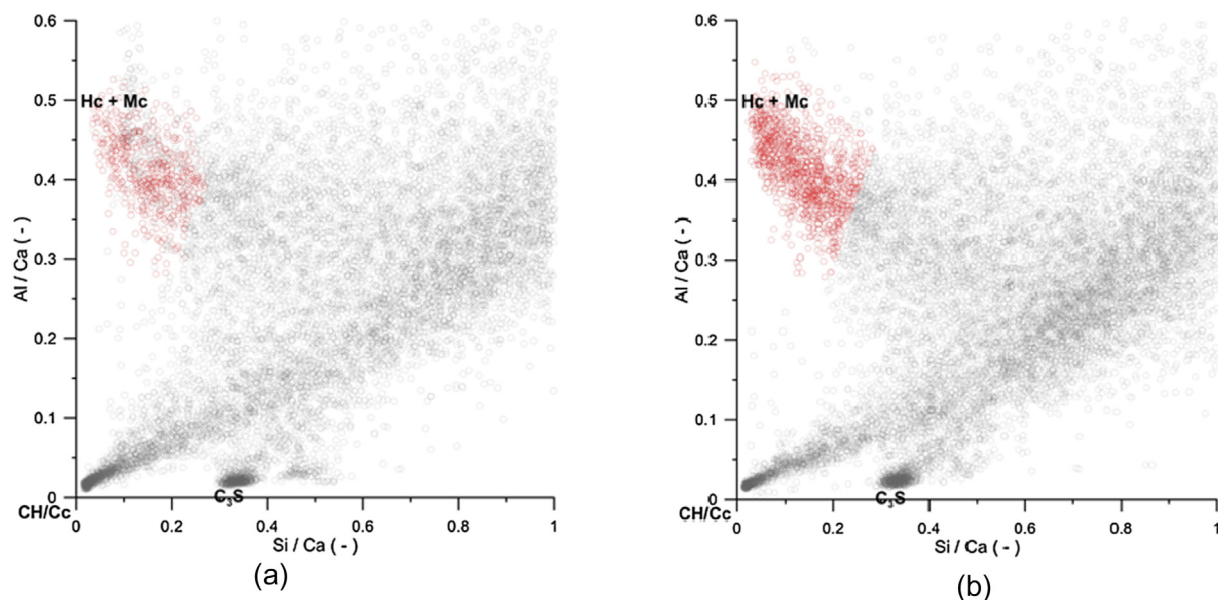
Fig. 13. Scatter plots of elemental ratios for the map collected for LC^3 no GA (a) and TEA 500 ppm (b) system at 7 days of hydration. AFm area is indicated.
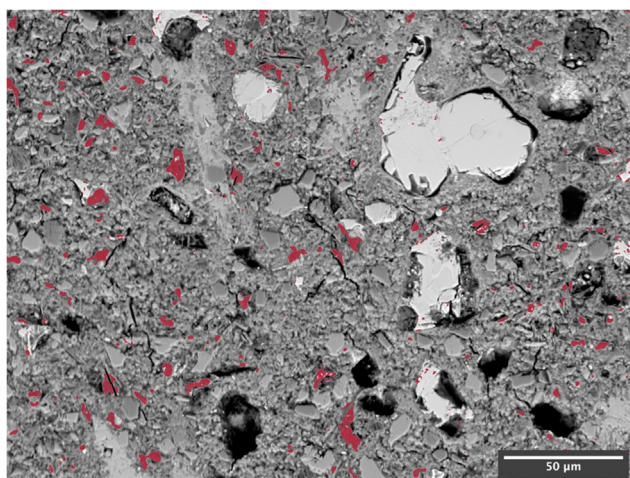

Fig. 14. Composite micrograph of LC^3 no GA showing Hc + Mc (red). Area fraction of AFm 2.3%. (For interpretation of the references to color in this figure legend, the reader is referred to the web version of this article.)

Fig. 15. Composite micrograph of LC^3 TEA 500 ppm showing Hc + Mc (red). Area fraction of AFm 6.2%. (For interpretation of the references to color in this figure legend, the reader is referred to the web version of this article.)

and Mc, which in turn increase the mechanical properties of the material. While more iron is put into solution, it appears to remain distributed rather than precipitate in hydrated phases.

4. Conclusions

This study evaluated the influence of different alkanolamines on the hydration, porosity and mechanical properties of LC^3. Special attention was given to TEA, as it showed to lead to the highest increase in compressive strength. Based on the results presented, the following conclusions can be drawn:

1. Alkanolamines have an enhancing effect on the aluminate reaction in LC^3 systems. A slight shortening of the time to reach the onset of the aluminate peak is observed for TEA and DEIPA at 200 ppm dosage due to an accelerated precipitation of ettringite. However, the amounts of ettringite observed at 24 h are similar among all systems as it is limited by the sulfate available.
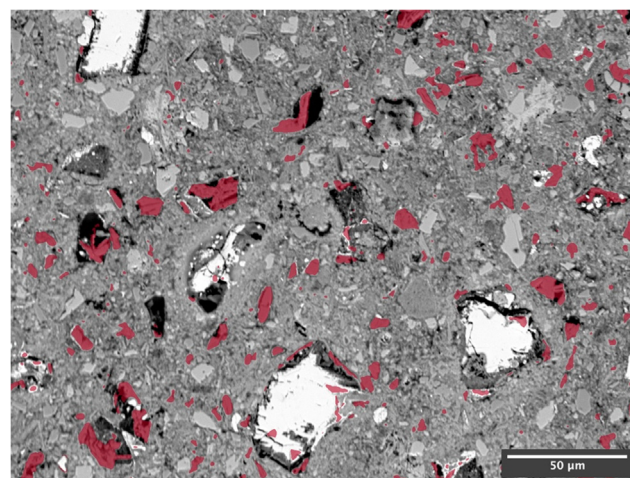
2. The addition of alkanolamines promote the hydration of ferrite and C$_3$A. In the case of TEA and DEIPA, an increase in the amount of Hc and Mc precipitated is observed, leading to a more refined porosity and an increase in compressive strength.

3. No decrease in the slope of the acceleration period is observed in LC^3 systems due to the addition of TEA up to 200 ppm, as the retardation effect over alite hydration is offset by the acceleration (filler) contribution of limestone and metakaolin. Higher dosages of TEA lead to decreasing rates of alite hydration. Dosages of TEA in the range of 2000 ppm may produce undersulfation of the system.

4. The addition of TEA in LC^3 leads to an increased amount of aluminum and iron in the pore solution at early age. The interaction of TEA with iron is mainly associated with an enhanced hydration of ferrite.

5. The rate of reaction of metakaolin is not significantly affected by the addition of TEA, independently of the iron content of the clay.

CRediT authorship contribution statement

Franco Zunino: Conceptualization, Methodology, Writing - original draft, Writing - review & editing. **Karen Scrivener:** Supervision, Writing - review & editing.

Declaration of Competing Interest

The authors declare that they have no known competing financial interests or personal relationships that could have appeared to influence the work reported in this paper.

Acknowledgements

Appendix A. Supplementary data

Supplementary data to this article can be found online at https://doi.org/10.1016/j.conbuildmat.2020.121293.

References

[1] K.L. Scrivener, V.M. John, E.M. Gartner, Eco-efficient cements: Potential economically viable solutions for a low-CO2 cement-based materials industry, Cem. Concr. Res. 114 (2018) 2–26.
[2] B. Lothenbach, K. Scrivener, R.D. Hooton, Supplementary cementitious materials, Cem. Concr. Res. 41 (12) (2011) 1244–1256.
[3] M. Schneider, M. Romer, M. Tschudin, H. Bolio, Sustainable cement production—present and future, Cem. Concr. Res. 41 (7) (2011) 642–650.
[4] K. Scrivener, F. Martirena, S. Bishnoi, S. Maity, Calcined clay limestone cements (LC3), Cem. Concr. Res. 114 (2018) 49–56.
[5] K. Scrivener, F. Avet, H. Maraghechi, F. Zunino, J. Ston, W. Hanpongpun, A. Favier, Impacting factors and properties of limestone calcined clay cements (LC3), Green Mater. 7 (1) (2019) 3–14.
[6] R. Fernandez, F. Martirena, K.L. Scrivener, The origin of the pozzolanic activity of calcined clay minerals: A comparison between kaolinite, illite and montmorillonite, Cem. Concr. Res. 41 (1) (2011) 113–122.
[7] M. Antoni, J. Rossen, F. Martirena, K. Scrivener, Cement substitution by a combination of metakaolin and limestone, Cem. Concr. Res. 42 (12) (2012) 1579–1589.
[8] A. Alujas, R. Fernández, R. Quintana, K.L. Scrivener, F. Martirena, Pozzolanic reactivity of low grade kaolinitic clays: Influence of calcination temperature and impact of calcination products on OPC hydration, Appl. Clay Sci. 108 (2015) 94–101.
[9] F. Zunino, K. Scrivener, Increasing the kaolinite content of raw clays using particle classification techniques for use as supplementary cementitious materials, Construction and Building Materials 244 (2020) 118335, https://doi.org/10.1016/j.conbuildmat.2020.118335.
[10] M. Cyr, P. Lawrence, E. Ringot, Efficiency of mineral admixtures in mortars: Quantification of the physical and chemical effects of fine admixtures in relation with compressive strength, Cem. Concr. Res. 36 (2) (2006) 264–277.
[11] P. Lawrence, M. Cyr, E. Ringot, Mineral admixtures in mortars effect of type, amount and fineness of fine constituents on compressive strength, Cement and Concrete Research 35 (6) (2005) 1092–1105.
[12] F. Zunino, M. Lopez, A methodology for assessing the chemical and physical potential of industrially sourced rice husk ash on strength development and early-age hydration of cement paste, Constr. Build. Mater. 149 (2017) 869–881.
[13] K. De Weerdt, Separate grinding versus intergrinding, SINTEF Report (2007).
[14] A. Pérez, A. Favier, K. Scrivener, F. Martirena, Influence Grinding Procedure, Limestone Content and PSD of Components on Properties of Clinker-Calcined Clay-Limestone Cements Produced by Intergrinding, Calcined Clays Sustain. Concr., Springer (2018) 358–365.
[15] J.J. Assaad, C.A. Issa, Effect of clinker grinding aids on flow of cement-based materials, Cement and Concrete Research 63 (2014) 1–11.
[16] M. Katsioti, P.E. Tsakiridis, P. Giannatos, Z. Tsibouki, J. Marinos, Characterization of various cement grinding aids and their impact on grindability and cement performance, Constr. Build. Mater. 23 (5) (2009) 1954–1959.
[17] S. Sohoni, R. Sridhar, G. Mandal, The effect of grinding aids on the fine grinding of limestone, quartz and Portland cement clinker, Powder Technol. 67 (3) (1991) 277–286.
[18] R.K. Mishra, D. Geissbuhler, H.A. Carmona, F.K. Wittel, M.L. Sawley, M. Weibel, et al., En route to a multi-model scheme for clinker comminution with chemical grinding aids, Adv. Appl. Ceram. 6753 (2015) 1–9, https://doi.org/10.1179/1743676115Y.0000000023.
[19] J. Cheung, A. Jeknavorian, L. Roberts, D. Silva, Impact of admixtures on the hydration kinetics of Portland cement, Cem. Concr. Res. 41 (12) (2011) 1289–1309.
[20] V.S. Ramachandran, Hydration of cement — role of triethanolamine, Cem. Concr. Res. 6 (5) (1976) 623–631.
[21] V.S. Ramachandran, Action of triethanolamine on the hydration of tricalcium aluminate, Cem. Concr. Res. 3 (1) (1973) 41–54.
[22] D. Heinz, M. Göbel, H. Hilbig, L. Urbonas, G. Bujauskaite, Effect of TEA on fly ash solubility and early age strength of mortar, Cem. Concr. Res. 40 (3) (2010) 392–397.
[23] J.-P. Perez, A. Nonat, S. Pourchet, S. Garrault, M. Mosquet, C. Canevet, Why TIPA leads to an Increase in the Mechanical Properties of Mortars Whereas TEA Does Not, ACI Mater. J. 217 (2003) 583–594.
[24] E. Gartner, D. Myers, Influence of Tertiary Alkanolamines on Portland Cement Hydration, J American Ceramic Society 76 (6) (1993) 1521–1530.
[25] S. Ma, W. Li, S. Zhang, Y. Hu, X. Shen, Study on the hydration and microstructure of Portland cement containing diethanol-isopropanolamine, Cem. Concr. Res. 67 (2015) 122–130.
[26] Y.L. Yaphary, Z. Yu, R.H.W. Lam, D. Lau, Effect of triethanolamine on cement hydration toward initial setting time, Constr. Build. Mater. 141 (2017) 94–103.
[27] K. Scrivener, R. Snellings, B. Lothenbach, A Practical Guide to Microstructural Analysis of Cementitious Materials, (2016) 540. doi:10.7693/wl20150205.
[28] F. Georget, edxia, Zenodo (2019), https://doi.org/10.5281/zenodo.3246902.
[29] F. Zunino, K.L. Scrivener, The influence of the sulfate requirement of blended cements, Cem. Concr. Res. 126 (2019), https://doi.org/10.1016/j.cemconres.2019.105918.
[30] F. Zunino, K.L. Scrivener, Factors influencing the sulfate balance in pure phase C3S/C3A systems, Cem. Concr. Res. (n.d.). Submitted.
[31] F. Zunino, K. Scrivener, Processing of calcined clays for applications in cementitious materials: The use of grinding aids and particle classification after grinding, in: Proc. Int. Conf. Sustain. Prod. Use Cem. Concr., Springer International Publishing, 2020. doi:10.1007/978-3-030-22034-1.
[32] F. Zunino, K. Scrivener, The reaction between metakaolin and limestone and its effect in porosity refinement and mechanical properties, Cem. Concr. Res. (n. d.).
[33] F. Zunino, Limestone calcined clay cements (LC3): raw material processing, sulfate balance and hydration kinetics, EPFL Thesis 8173, 2020.
[34] François Avet, Ruben Snellings, Adrian Alujas Diaz, Mohsen Ben Haha, Karen Scrivener, Development of a new rapid, relevant and reliable (R3) test method to evaluate the pozzolanic reactivity of calcined kaolinitic clays, Cem. Concr. Res. 85 (2016) 1–11.